Nuclear Engineering and Technology 55 (2023) 1563–1570

Contents lists available at ScienceDirect

Nuclear Engineering and Technology

journal homepage: www.elsevier.com/locate/net

Technical Note

Establishment of DeCART/MIG stochastic sampling code system and Application to UAM and BEAVRS benchmarks

Ho Jin Park [a, *], Jin Young Cho [b]

[a] Kyung Hee University, 1732, Deogyeong-daero, GiHeung-gu, Yongin-si, Gyeonggi-do, South Korea
[b] Korea Atomic Energy Research Institute, 111, Daedeok-daero 989beon-gil, Daejeon, South Korea

ARTICLE INFO

Article history:
Received 15 December 2022
Received in revised form
16 February 2023
Accepted 17 February 2023
Available online 20 February 2023

Keywords:
Stochastic sampling
Uncertainty quantification
Cross section sampling
DeCART
MIG
UAM
BEAVRS

ABSTRACT

In this study, a DeCART/MIG uncertainty quantification (UQ) analysis code system with a multi-correlated cross section stochastic sampling (S.S.) module was established and verified through the UAM (Uncertainty Analysis in Modeling) and the BEAVRS (Benchmark for Evaluation And Validation of Reactor Simulations) benchmark calculations. For the S.S. calculations, a sample of 500 DeCART multi-group cross section sets for two major actinides, i.e., ^{235}U and ^{238}U, were generated by the MIG code and covariance data from the ENDF/B-VII.1 evaluated nuclear data library. In the three pin problems (i.e. TMI-1, PB2, and Koz-6) from the UAM benchmark, the uncertainties in k_{inf} by the DeCART/MIG S.S. calculations agreed very well with the sensitivity and uncertainty (S/U) perturbation results by DeCART/MUSAD and the S/U direct subtraction (S/U-DS) results by the DeCART/MIG. From these results, it was concluded that the multi-group cross section sampling module of the MIG code works correctly and accurately. In the BEAVRS whole benchmark problems, the uncertainties in the control rod bank worth, isothermal temperature coefficient, power distribution, and critical boron concentration due to cross section uncertainties were calculated by the DeCART/MIG code system. Overall, the uncertainties in these design parameters were less than the general design review criteria of a typical pressurized water reactor start-up case. This newly-developed DeCART/MIG UQ analysis code system by the S.S. method can be widely utilized as uncertainty analysis and margin estimation tools for developing and designing new advanced nuclear reactors.
© 2023 Korean Nuclear Society, Published by Elsevier Korea LLC. This is an open access article under the CC BY-NC-ND license (http://creativecommons.org/licenses/by-nc-nd/4.0/).

1. Introduction

Innovative and challenging nuclear reactors have been successively proposed and developed to achieve more improved safety, efficiency, and sustainability. In particular, from a safety standpoint, it is extremely crucial to analyze the uncertainties of the design and to secure enough margins for nuclear design parameters in a new type of nuclear reactor. Accordingly, general regulating agencies has issued a construction permit or an operating license through the full verification and validation (V&V) of the uncertainty quantification (UQ) tools or methodologies, which are used in new types of nuclear reactor designs. The Korea Atomic Energy Research Institute (KAERI) has developed its own two-step neutronic core design code system that uses the DeCART2D [1] (Deterministic Core Analysis based on Ray Tracing) two-dimensional lattice neutron/photon transport code and the MASTER [2] whole core nodal diffusion code. Moreover, KAERI has developed the DeCART [3] three-dimensional (3D) method of characteristics (MOC) neutron/photon transport code for direct whole-core calculations. The DeCART2D/MASTER two-step code system and the DeCART whole core analysis code have been utilized as tools for new nuclear reactor core designs since the early 2000s. In general, the uncertainties of the codes for the nuclear core design and analysis have been calculated under conservative conditions. According to this conservative approach, the uncertainties of the design parameters are defined using the tolerance limits with 95% probability and 95% confidence. In 2017, the uncertainties of the DeCART2D/MASTER two-step nuclear core design code system were evaluated for the axially integrated fuel assembly power and fuel rod power, as well as the individual and total rod worth [4]. However, this conservative approach may lead to extra costs from unrealistic calculation conditions and excessive designer-defined margins. To avoid the disadvantage of the conservative approach,

* Corresponding author. Kyung Hee University, 1732, Deogyeong-daero, GiHeung-gu, Yongin-si, Gyeonggi-do, 17104, South Korea.
E-mail address: parkhj@khu.ac.kr (H.J. Park).

https://doi.org/10.1016/j.net.2023.02.027
1738-5733/© 2023 Korean Nuclear Society, Published by Elsevier Korea LLC. This is an open access article under the CC BY-NC-ND license (http://creativecommons.org/licenses/by-nc-nd/4.0/).

the Best Estimate Plus Uncertainty (BEPU) method [5] has been constructed to estimate the uncertainty quantification (UQ) of nuclear core design and analysis codes.

In the BEPU method, there are two major streams to estimate the output uncertainties due to input uncertainties (e.g., nuclear data, tolerance, material composition), which have been developed through various studies [6–11]. One major stream is the sensitivity/uncertainty (S/U) analysis method based on the perturbation techniques. KAERI developed the MUSAD (Modules for Uncertainty and Sensitivity Analysis for DeCART) code [12,13] for the DeCART S/U analysis. The MUSAD code is based on the classical and generalized perturbation theories. KAERI has applied the DeCART/MUSAD code system to the UQ analysis of various VHTR systems such as PMR-200 and MHTGR-350.

The other major stream is the stochastic or statistical sampling (S.S.) method, which is the so-called Brute Force method. In the S.S. method, the input parameters are randomly sampled while considering their averages, variances, and correlations between them. Using each sampled input parameter, the output parameters are calculated by a program or a code. Recently, KAERI developed the multi-correlated nuclear cross section sampling code MIG and established the S.S. method based on the McCARD/MIG UQ analysis code system [14].

The main goal of this study was to establish and validate the S.S. method-based DeCART/MIG UQ analysis code system. For the V&V of the DeCART/MIG UQ code system, the uncertainty analysis in modeling (UAM) [15,16] benchmark and BEAVRS [17] benchmark calculations were performed using the covariance data in the ENDF/B-VII.1 evaluated nuclear cross section library [18]. Section II explains the overview of the newly-established DeCART/MIG S.S. code system for the UQ analysis. In Section III, the DeCART/MIG S.S. code system is verified and validated through the UQ analysis of the UAM benchmark pin problems and the BEAVRS whole core problem. The conclusions are given in Section IV.

2. Uncertainty quantification analysis by the DeCART/MIG code system

2.1. DeCART/MIG cross section sampling code system

In this study, the DeCART/MIG cross section sampling code system was established using the up-to-date MIG code (i.e. version 1.7) and DeCART (i.e. version 3.0). The MIG 1.7 code has the capability to perform multiple-correlated sampling to estimate the uncertainties of nuclear reactor core design parameters due to nuclear data uncertainties. The Cholesky covariance matrix decomposition module for multiple-correlated random sampling was implemented into the MIG code. As shown in Eq. (1), a lower triangular matrix $\mathbf{B}$ and the transpose matrix of $\mathbf{B}$, $\mathbf{B}^T$ can be calculated by the Cholesky decomposition of the nuclear reaction cross section covariance matrix $\mathbf{C}_u$.

$$\mathbf{C}_u = \mathbf{B}\cdot\mathbf{B}^T \tag{1}$$

Then, if $\mathbf{C}_u$ is symmetrical and positive definite, a i-th sample value $\mathbf{X}^i$ can be calculated by

$$\mathbf{X}^i = \overline{\mathbf{X}} + \mathbf{B}\cdot\mathbf{Z}, \tag{2}$$

where $\overline{\mathbf{X}}$ and $\mathbf{Z}$ are the mean cross section vector and a random normal vector calculated by the Box-Muller method [19].

Fig. 1 shows the flowchart of the DeCART/MIG nuclear cross section UQ analysis code system based on the S.S. method. First, the MIG 1.7 code can generate sampled cross section sets by using multi-group covariance data from an evaluated nuclear cross section library and an MIG input file. In this study, a multi-group cross section relative covariance matrix was prepared by the ERRORR module of the NJOY code [20] that used ENDF/B-VII.1 evaluated nuclear data library [18]. The DeCART 47 energy group structure for the ENDF/B-VII.1 covariance data was adopted for both the cross-section covariance matrix and the sampled cross section sets. The raw covariance data were edited and reformulated by the MIG code to be used in the DeCART transport calculations. The MIG code has the capability to process a relative covariance matrix and its associated average multi-group cross sections and then convert them into the covariance matrix $\mathbf{C_u}$ as specified in Eq. (2). Through the sampling process, the 500 sampled cross section sets from the ENDF/B-VII.1 covariance data for the two major actinide isotopes (i.e. ^{235}U and ^{238}U), ^{1}H, and ^{16}O were generated for the DeCART/MIG UQ calculations. The samplings were conducted on the 47-group cross sections and the corresponding 47-group covariance matrix in multi-group representation. In the UQ procedure, the MIG code generates base-to-sampled cross section ratios and the DeCART code generates the final sampled cross sections by the product of the base-to-sampled cross section ratio and the existing self-shielded cross section from the DeCART library. In the DeCART code, the module for reading the sampled cross section ratios and generating the final sampled cross section was newly implemented. Meanwhile, the sampling process for the DeCART 47-group cross sections can be performed using both individual and compounded covariance matrix. The DeCART code can only read the compounded absorption and scattering cross sections from its library to solve the Boltzmann transport equations instead of the cross sections for an individual reaction type (i.e. capture, fission, (n,2n), (n,3n), elastic scattering, and inelastic scattering cross section). The compounded covariance matrix for the scattering cross section can be provided by elastic (MT2) and inelastic (MT4) scattering cross sections as shown in Eqs. (3) and (4):

$$\begin{aligned}\mathrm{cov}[\sigma_{s,g},\sigma_{s,g'}] =& \mathrm{cov}[\sigma_{e,g},\sigma_{e,g'}] + \mathrm{cov}[\sigma_{i,g},\sigma_{i,g'}] + 4\mathrm{cov}[\sigma_{2n,g},\sigma_{2n,g'}] + 9\mathrm{cov}[\sigma_{3n,g},\sigma_{3n,g'}] + \mathrm{cov}[\sigma_{e,g},\sigma_{i,g'}] + 2\mathrm{cov}[\sigma_{e,g},\sigma_{2n,g'}] \\ &+ 3\mathrm{cov}[\sigma_{e,g},\sigma_{3n,g'}] + \mathrm{cov}[\sigma_{i,g},\sigma_{e,g'}] + 2\mathrm{cov}[\sigma_{i,g},\sigma_{2n,g'}] + 3\mathrm{cov}[\sigma_{i,g},\sigma_{3n,g'}] + 2\mathrm{cov}[\sigma_{2n,g},\sigma_{e,g'}] + 2\mathrm{cov}[\sigma_{2n,g},\sigma_{i,g'}] \\ &+ 6\mathrm{cov}[\sigma_{2n,g},\sigma_{3n,g'}] + 3\mathrm{cov}[\sigma_{3n,g},\sigma_{e,g'}] + 3\mathrm{cov}[\sigma_{3n,g},\sigma_{i,g'}] + 6\mathrm{cov}[\sigma_{3n,g},\sigma_{2n,g'}]\end{aligned} \tag{3}$$

$$\sigma_{s,g} = \sigma_{e,g} + \sigma_{i,g} + 2\sigma_{2n,g} + 3\sigma_{3n,g} \tag{4}$$

where $\sigma_{e,g}$, $\sigma_{i,g}$, $\sigma_{2n,g}$, and $\sigma_{3n,g}$ indicate the g-th group elastic scattering, inelastic scattering, (n,2n), and (n,3n) nuclear reaction cross section. In the same manner, the compounded covariance matrix for the absorption cross section can be expressed by

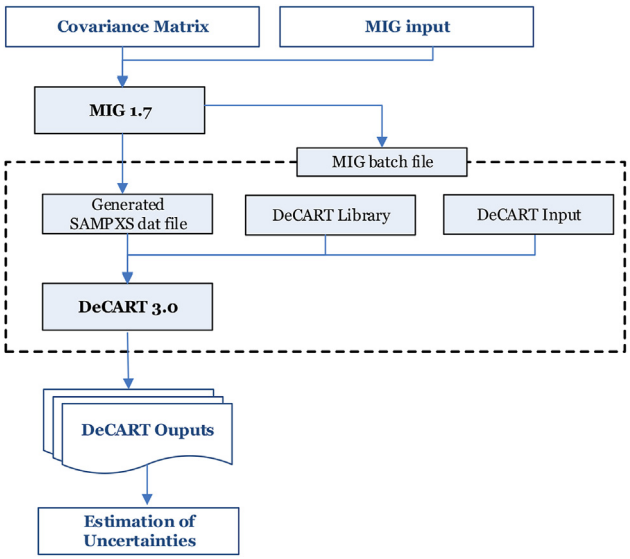

Fig. 1. Flowchart of DeCART/MIG nuclear cross section UQ analysis code system.

$$\begin{aligned}\mathrm{cov}\left[\sigma_{a,g},\sigma_{a,g'}\right] &= \mathrm{cov}\left[\sigma_{\gamma,g},\sigma_{\gamma,g'}\right]+\mathrm{cov}\left[\sigma_{f,g},\sigma_{f,g'}\right]+\mathrm{cov}\left[\sigma_{2n,g},\sigma_{2n,g'}\right]+4\mathrm{cov}\left[\sigma_{3n,g},\sigma_{3n,g'}\right]\\ &+\mathrm{cov}\left[\sigma_{\gamma,g},\sigma_{f,g'}\right]-\mathrm{cov}\left[\sigma_{\gamma,g},\sigma_{2n,g'}\right]-2\mathrm{cov}\left[\sigma_{\gamma,g},\sigma_{3n,g'}\right]+\mathrm{cov}\left[\sigma_{f,g},\sigma_{\gamma,g'}\right]\\ &-\mathrm{cov}\left[\sigma_{f,g},\sigma_{2n,g'}\right]-2\mathrm{cov}\left[\sigma_{f,g},\sigma_{3n,g'}\right]-\mathrm{cov}\left[\sigma_{2n,g},\sigma_{\gamma,g'}\right]-\mathrm{cov}\left[\sigma_{2n,g},\sigma_{f,g'}\right]\\ &+2\mathrm{cov}\left[\sigma_{2n,g},\sigma_{3n,g'}\right]-2\mathrm{cov}\left[\sigma_{3n,g},\sigma_{\gamma,g'}\right]-2\mathrm{cov}\left[\sigma_{3n,g},\sigma_{f,g'}\right]+2\mathrm{cov}\left[\sigma_{3n,g},\sigma_{2n,g'}\right] \end{aligned} \tag{5}$$

$$\sigma_{a,g}=\sigma_{\gamma,g}+\sigma_{f,g}-\sigma_{2n,g}-2\sigma_{3n,g} \tag{6}$$

where $\sigma_{\gamma,g}$, $\sigma_{f,g}$ are the g-th group (n, γ), fission cross section, respectively. After the nuclear cross section sampling processes of the MIG code finished, the DeCART neutronic transport calculations were performed using each sampled cross section set. Finally, the statistical analyses were performed on the DeCART results to determine the uncertainties of the target design parameters due to the cross-section uncertainties.

2.2. DeCART/MIG uncertainty quantification analysis by direct subtraction method

Equation (7) shows a common S/U analysis equation (i.e., the sandwich equation) for the uncertainty quantification of an output parameter Q due to uncertain input parameters (i.e., $x_{k'}$ and $x_{k''}$).

$$\begin{aligned}\sigma^2[Q] &= \lim_{N\to\infty}\frac{1}{N-1}(Q_k-\overline{Q})^2\\ &\cong \lim_{N\to\infty}\frac{1}{N-1}\left(\sum_{k'}\sum_{k''}(x_{k'}-\overline{x_{k'}})(x_{k''}-\overline{x_{k''}})\cdot\frac{\partial\overline{Q}}{\partial x_{k'}}\cdot\frac{\partial\overline{Q}}{\partial x_{k''}}\right)\end{aligned} \tag{7}$$

This involves a first-order Taylor series expansion about the uncertain input parameters. Accordingly, S/U analysis equations have sensitivity coefficients and covariance data. In the deterministic S/U analysis, the sensitivity coefficients ($\partial\overline{Q}/\partial x_{k'}$ and $\partial\overline{Q}/\partial x_{k''}$) are generally calculated by the perturbation technique. Meanwhile, the direct subtraction calculations can be adopted as an alternative way to obtain the sensitivity coefficients. To apply of the direct subtraction calculations, the sensitivity coefficients can be approximated as

$$\frac{\partial\overline{Q}}{\partial x_{k'}}=\frac{\partial\overline{Q}(x_{k'}+\sigma(x_{k'}))-\partial\overline{Q}(x_{k'})}{\sigma(x_{k'})} \tag{8}$$

The perturbed term $\partial\overline{Q}(x_{k'}+\sigma(x_{k'}))$ and reference term $\partial\overline{Q}(x_{k'})$ about $x_{k'}$ can be calculated by the two direct calculations. The S/U-DS method is intuitive and very easy to implement. However, the S/U analyses with the direct subtraction (S/U-DS) need the higher number of calculations as the number of input parameters than the perturbation method. Nevertheless, the best benefit of the S/U-DS method is that one can obtain accurate S/U analysis solutions and it can be used as reference. In this study, the S/U-DS analysis modules were implemented into the DeCART/MIG code system.

3. Validation and application of DeCART/MIG stochastic sampling code system

3.1. Validation by the UAM exercise I-1 benchmark

To validate the newly-established DeCART/MIG UQ code system, the Uncertainty Analysis in Modelling (UAM) Exercise I-1 benchmark [15,16] was considered. The UAM benchmark set is proposed by the Organization for Economic Co-operation and Development (OECD), the expert group of the Nuclear Energy Agency (NEA), to estimate the uncertainties in the nuclear reactor physics and thermal/hydraulic (T/H) calculations for light water reactor (LWR) design and analysis. In this study, we selected three UAM Exercise I-1 benchmark hot full power (HFP) pin problems for the pressurized water reactor (PWR) based Three Mile Island Unit 1 (TMI-1), the Boiling Water Reactor (BWR) based Peach Bottom Unit 2 (PB-2), and the VVER-1000 reactor based Kozloduy-6 (Koz-6) problem. Table 1 shows the brief configurations of the three UAM HFP pin problems.

All UQ analysis for the UAM pin problems were conducted using the DeCART ENDF/B-VII.1 based cross section library and the prepared 500 cross section sample sets for ^{1}H, ^{16}O, ^{235}U, and ^{238}U. The five-batch calculations with the 100 cross section sample sets per batch were conducted to estimate the range of the uncertainties of output results due to the uncertainties of the cross sections. In this study, the sampled elastic and inelastic scattering cross section sets were provided by the individual covariance matrix option, not the compounded one because it is already confirmed that there are no significant differences between two covariance matrix options. In the sampled cross section sets, ν, capture, (n,2n), (n,3n), fission, elastic and inelastic scattering reaction cross sections, and fission spectrum were considered.

Table 2 and Fig. 2 present the uncertainties in k_{inf} for the TMI-1 HFP pin problem for each reaction. In the DeCART/MIG S.S. results,

Table 1
Configuration of the HFP pins in the UAM benchmark problem.

Parameter	TMI-1 HFP	PB2 HFP	Koz-6 HFP
Pin Pitch (cm)	1.4427	1.875	1.275
Fuel Pellet Radius (cm)	0.46955	0.60579	0.378[a]
Cladding Inner Radius (cm)	0.4791	0.62103	0.386
Cladding Outer Radius (cm)	0.5464	0.71501	0.455
Fuel/Cladding/Moderator Material	UO_2/ Zircaloy-4/H_2O	UO_2/ Zircaloy-2/H_2O	UO_2/ Zr+1%Nb/H_2O
^{235}U Enrichment (w/o)	4.85	2.93	3.3
Fuel/Cladding/Moderator Temperature (K)	900/600/562	900/600/557	900/600/560

[a] Koz-6 has a central void region with 1.4 mm diameter in the fuel pellet.

the total k_{inf} uncertainty due to the ^{235}U and ^{238}U cross section uncertainties, including fission spectrum, was about 1086 pcm (0.78%). The largest contributions for each isotope were ^{235}U ν (849 pcm, 0.61%) and ^{238}U (n,γ) cross section (550 pcm, 0.39%). It is worthwhile to note that there were significant contributions from the ^{235}U fission spectrum uncertainties (214 pcm, 0.15%). Table 3 and Fig. 3 present the uncertainties in k_{inf} for the PB2 HFP pin problem. The total uncertainty in k_{inf} due to the ^{235}U and ^{238}U cross section uncertainties was 1059 pcm (0.89%). In the same manner as the TMI-1 HFP pin problem, the largest contributions were the ^{235}U ν (691 pcm, 0.58%) and ^{238}U (n,γ) cross section (692 pcm, 0.58%). Table 4 and Fig. 4 show the uncertainties in k_{inf} for the Koz-6 HFP pin problem. The total uncertainty in k_{inf} was 1076 pcm (0.81%). For comparison, the DeCART/MUSAD [9] and DeCART/MIG S/U-DS results are provided for each UAM benchmark problem. Overall, the uncertainties in k_{inf} by the DeCART/MIG S.S. and others were in good agreement when considering their statistical uncertainties. It was observed that there were comparable differences between the uncertainties of DeCART/MUSAD and others due to the uncertainties of the fission spectrum and ^{238}U (n,γ) cross section. In this particular case, the detailed validation for the cross-section sampling sets will be conducted in the future. From these results, it was confirmed that the DeCART/MIG UQ analysis code systems work well for all the UAM exercise I-1 problems.

The DeCART/MIG code system utilizes self-shielded multi-group cross sections generated by the external code system. However, performing uncertainty analysis with these pre-self-shielded cross sections leads to discrepancies with the covariance data from evaluated nuclear data files, which are based on infinitely-diluted cross sections. As such, the uncertainty change resulting from the resonance treatment should be considered as an implicit

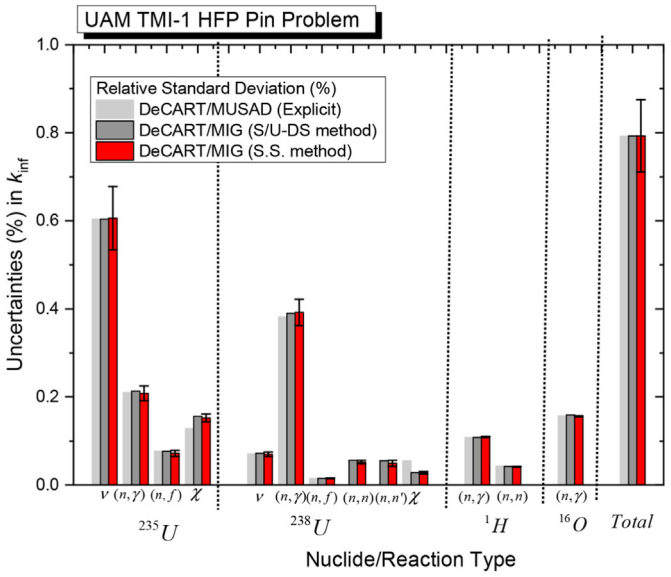

Fig. 2. Comparison between the uncertainties in the k_{inf} by the DeCART/MIG and DeCART/MUSAD for the UAM TMI-1 HFP pin problem.

Table 2
Uncertainties in the k_{inf} for UAM TMI-1 pin problem.

Nuclide	Reaction Type	MT Number	Uncertainties in the k_{inf} (%)		
			DeCART/MUSAD	DeCART/MIG	
			S/U	S/U-DS	S·S.
^{235}U	ν	452	0.604	0.604	0.606 ± 0.032
	(n,γ)	102	0.210	0.213	0.208 ± 0.007
	(n,f)	18	0.077	0.077	0.072 ± 0.003
	(n,n)	2	–	0.001	0.001 ± 0.001
	(n,n')	4	–	0.001	0.001 ± 0.001
	χ	1018	0.128	0.156	0.152 ± 0.004
^{238}U	ν	452	0.071	0.072	0.070 ± 0.002
	(n,γ)	102	0.382	0.390	0.392 ± 0.013
	(n,f)	18	0.015	0.015	0.015 ± 0.001
	(n,n)	2	–	0.056	0.052 ± 0.002
	(n,n')	4	–	0.055	0.049 ± 0.003
	χ	1018	0.055	0.028	0.028 ± 0.001
^{1}H	(n,γ)	102	0.108	0.108	0.109 ± 0.001
	(n,n)	2	0.043	0.042	0.041 ± 0.001
^{16}O	(n,γ)	102	0.157	0.159	0.156 ± 0.001
	(n,n)	2	0.002	0.002	0.002 ± 0.001
^{235}U+^{238}U (w/o χ)			0.761	0.765	0.762 ± 0.032
^{235}U+^{238}U (w/χ)			0.774	0.775	0.781 ± 0.041
Total			0.792	0.793	0.793 ± 0.036

Table 3
Uncertainties in the k_{inf} for UAM PB2 pin problem.

Nuclide	Reaction Type	MT Number	Uncertainties in the k_{inf} (%)		
			DeCART/MUSAD	DeCART/MIG	
			S/U	S/U-DS	S·S.
^{235}U	ν	451	0.582	0.580	0.581 ± 0.032
	(n,γ)	102	0.192	0.190	0.191 ± 0.006
	(n,f)	18	0.091	0.091	0.080 ± 0.003
	(n,n)	2	–	0.001	0.001 ± 0.001
	(n,n')	4	–	0.001	0.001 ± 0.001
	χ	1018	0.214	0.254	0.250 ± 0.006
^{238}U	ν	451	0.107	0.111	0.108 ± 0.002
	(n,γ)	102	0.539	0.581	0.582 ± 0.020
	(n,f)	18	0.025	0.027	0.027 ± 0.001
	(n,n)	2	–	0.128	0.122 ± 0.003
	(n,n')	4	–	0.125	0.116 ± 0.007
	χ	1018	0.108	0.073	0.073 ± 0.003
^{1}H	(n,γ)	102	0.096	0.095	0.098 ± 0.001
	(n,n)	2	0.056	0.056	0.056 ± 0.001
^{16}O	(n,γ)	102	0.164	0.167	0.164 ± 0.001
	(n,n)	2	0.004	0.004	0.004 ± 0.001
^{235}U+^{238}U (w/o χ)			0.836	0.842	0.860 ± 0.035
^{235}U+^{238}U (w/χ)			0.870	0.861	0.891 ± 0.049
Total			0.884	0.898	0.889 ± 0.041

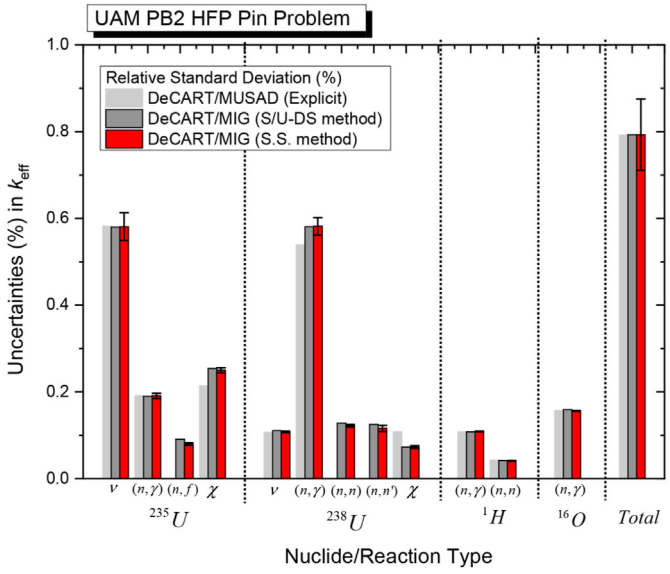

Fig. 3. Comparison between the uncertainties in the k_{inf} by the DeCART/MIG and DeCART/MUSAD for the UAM PB2 HFP pin problem.

uncertainty. The MUSAD code can generate an implicit uncertainty using multi-group self-shielding factors [13]. Table 5 shows the implicit and explicit uncertainties in k_{inf} due to the total and ^{238}U capture cross section uncertainties for the UAM pin problems. It is noted that the explicit uncertainties due to ^{238}U capture cross section were overestimated compared to 16–19% with the implicit uncertainties and the total explicit uncertainties were found to be 4–6% higher than the total implicit uncertainties. Moreover, the implicit effects on the other isotopes and reactions were tested and it was observed that there are no significant differences between them.

3.2. Nuclear data UQ analysis for the BEAVRS benchmark

The BEAVRS benchmark [17] provides a highly-detailed PWR specification with two-cycles of measured operation data such as control rod bank worth (CRBW), isothermal temperature coefficient (ITC), fuel assembly (FA)-wise detector signals, and critical boron concentrations (CBCs) with two-cycles burnup. The UQ analyses for the BEAVRS benchmark were conducted by the DeCART/MIG UQ analysis code system with the ENDF/B-VII.1 based prepared cross section sample sets for the ^{235}U and ^{238}U isotopes. The same multi-group cross section library and cross section sample sets as the ones used in the UAM benchmark were utilized for the BEAVRS benchmark.

Table 6 shows the uncertainties in the CRBW of Cycle 1 due to the ^{235}U and ^{238}U cross section uncertainties. The maximum relative uncertainties of the individual and total CRBWs due to the cross-section uncertainties were 2.5% and 0.6%. The general design review criteria (DRC) [21,22] of the individual and total CRBWs on start-up and operation were 10% and 15%, respectively. Therefore, it was observed that the uncertainties in the CRBWs by the DeCART/MIG calculations were less than the DRC of CRBW in a typical PWR start-up case. Fig. 5 shows the FA-wise power distributions for the hot-zero power (HZP) condition. In Fig. 5, the first and second lines indicate the normalized FA-wise power distribution for the measurement and DeCART/MIG S.S. calculations, whereas the third line means the uncertainties due to the ^{235}U and ^{238}U cross section uncertainties. It was observed that the maximum uncertainty of the FA-wise power distribution was 1.3% at the central H-8 FA. The DRC of the FA-wise power distribution was 10% in a typical PWR start-up case. In the same manner, the uncertainties in the FA-wise power distribution were less than the DRC values. Table 7 shows the uncertainties in the ITCs due to the ^{235}U and ^{238}U cross section uncertainties. The maximum uncertainty of the ITC for each case was 0.20 pcm/^{o}F, which was also less than the DRC values (2.0 pcm/^{o}F).

Tables 8 and 9 provide the average CBCs and their uncertainties due to the ^{235}U and ^{238}U cross section uncertainties for the two-cycle burnup. The DRC of the CBC was 50 pcm. The uncertainties in the CBC due to the ^{235}U and ^{238}U cross section uncertainties ranged from 5.5 pcm to 55.3 pcm. At the beginning of the cycle (BOC) in Cycles 1 and 2, the CBC uncertainty was slightly larger than the DRC value (50 ppm) at the All Rod Out (ARO) state. However, as the burnup proceed, the CBC uncertainty quickly dropped to less than the DRC value. Figs. 6 and 7 plot the average CBCs and their uncertainties due to the ^{235}U and ^{238}U cross section uncertainties for Cycles 1 and 2, respectively. The black box points mean the

Table 4
Uncertainties in the k_{inf} for UAM Koz-6 pin problem.

Nuclide	Reaction Type	MT Number	Uncertainties in the k_{inf} (%)		
			DeCART/MUSAD	DeCART/MIG	
			S/U	S/U-DS	S·S.
^{235}U	ν	451	0.619	0.620	0.622 ± 0.035
	(n,γ)	102	0.186	0.186	0.186 ± 0.006
	(n,f)	18	0.093	0.093	0.085 ± 0.004
	(n,n)	2	–	0.001	0.001 ± 0.001
	(n,n')	4	–	0.001	0.001 ± 0.001
	χ	1018	0.131	0.157	0.153 ± 0.004
^{238}U	ν	451	0.072	0.073	0.071 ± 0.001
	(n,γ)	102	0.440	0.438	0.441 ± 0.016
	(n,f)	18	0.016	0.017	0.016 ± 0.001
	(n,n)	2	–	0.052	0.050 ± 0.001
	(n,n')	4	–	0.051	0.047 ± 0.003
	χ	1018	0.056	0.029	0.028 ± 0.001
^{1}H	(n,γ)	102	0.148	0.148	0.149 ± 0.001
	(n,n)	2	0.042	0.042	0.042 ± 0.001
^{16}O	(n,γ)	102	0.078	0.078	0.078 ± 0.001
	(n,n)	2	0.003	0.001	0.003 ± 0.001
^{235}U+^{238}U (w/o χ)			0.799	0.798	0.794 ± 0.032
^{235}U+^{238}U (w/χ)			0.812	0.814	0.810 ± 0.041
Total			0.824	0.834	0.824 ± 0.027

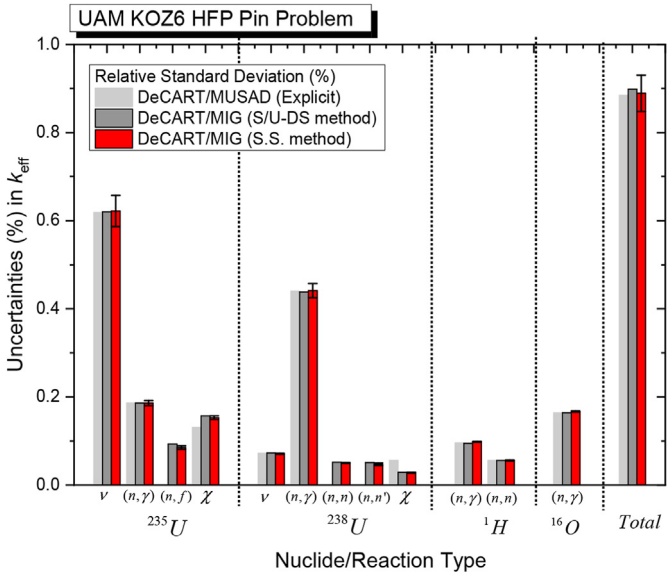

Fig. 4. Comparison between the uncertainties in the k_{inf} by the DeCART/MIG and DeCART/MUSAD for the UAM Koz-6 HFP pin problem.

Table 5
Explicit and Implicit Uncertainties in the k_{inf} for UAM pin benchmarks.

Benchmark	Reaction Type	MT Number	Uncertainties in the k_{inf} (%)		
			DeCART/MUSAD		DeCART/MIG
			Explicit	Explicit+Implicit	Explicit
TMI-1	(n,γ)	102	0.382	0.310	0.392 ± 0.013
	Total		0.792	0.764	0.793 ± 0.036
PB-2	(n,γ)	102	0.539	0.441	0.582 ± 0.020
	Total		0.884	0.828	0.889 ± 0.041
Koz-6	(n,γ)	102	0.440	0.369	0.441 ± 0.016
	Total		0.824	0.788	0.824 ± 0.027

Table 6
Uncertainties in the control rod bank worth due to the ^{235}U and ^{238}U cross section uncertainties (Cycle 1).

Case	CRBW and its uncertainties		
	Average (pcm)	Unc. (pcm)[a]	Rel. Unc. (%)[a]
D in	781	5	0.7
D, C in	1246	8	0.6
D, C, B in	1252	13	1.0
D, C, B, A in	499	12	2.5
D, C, B, A, SE in	458	10	2.1
Total	4236	24	0.6

[a] Unc.(pcm) and Rel. Unc.(%) are the absolute and relative uncertainties in the CRBW due to cross section uncertainties.

average CBCs by the DeCART/MIG S.S. calculations whereas their error bars indicate their uncertainties due to the ^{235}U and ^{238}U cross section uncertainties. The red cycle points represent the measurements from the reference with their error bars representing the DRC value (=50 ppm) for comparison. As shown in Figs. 6 and 7, it was observed that all the measured values were distributed within the uncertainties due to the ^{235}U and ^{238}U cross section uncertainties by the DeCART/MIG S.S. calculations.

4. Conclusions

In this study, the multi-correlated variable random sampling code, MIG, was successfully updated for the sampling process of the DeCART cross section library. In addition, the DeCART/MIG UQ analysis code system was established and verified through the UAM benchmark exercise I-1 pin problems and the BEAVRS whole core benchmark problems. To validate this DeCART/MIG UQ analysis code system, a S/U analysis module based on the direct subtraction was additionally implemented into the MIG code. For the S.S. calculations in the DeCART code, the 500 cross section sample sets for the two major isotopes - ^{235}U and ^{238}U from the ENDF/B-VII.1 covariance data were generated by the MIG code. In the three pin problems (i.e., the TMI-1, PB2, and Koz-6) from the UAM

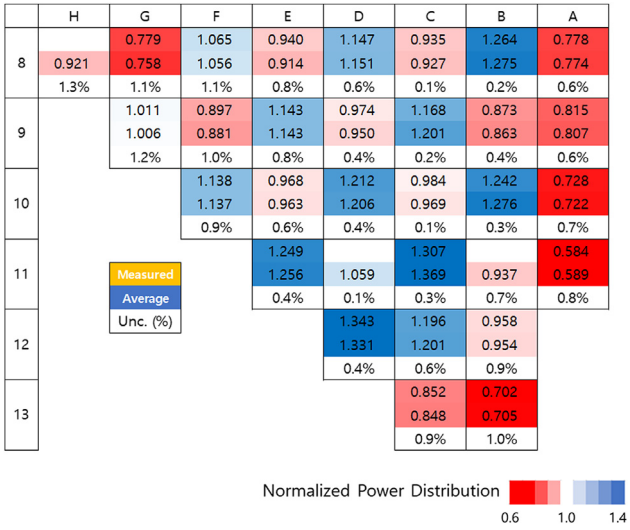

Fig. 5. Uncertainties of the assembly-wise power distribution due to the ^{235}U and ^{238}U cross section uncertainties.

Table 7
Uncertainties in the isothermal temperature coefficients due to the ^{235}U and ^{238}U cross section uncertainties.

Case	ITC and its uncertainties		
	Average (pcm/°F)	Unc. (pcm/°F)[a]	Rel. Unc. (%)[a]
ARO	−3.13	0.19	6.24
D in	−4.57	0.20	4.41
D, C in	−9.51	0.20	2.14

[a] Unc.(pcm/°F) and Rel. Unc.(%) are the absolute and relative uncertainties in the ITC due to cross section uncertainties.

benchmark, the uncertainties in the k_{inf} by the DeCART/MIG S.S. calculations agreed very well with the S/U perturbation method based DeCART/MUSAD and the S/U direct subtraction based DeCART/MIG results. From these results, it was concluded that the multi-group cross section sampling module of the MIG code works correctly and accurately. However, it was observed that there are comparable differences between the DeCART/MUSAD results and the others in the fission spectrum and ^{238}U (n,γ) cross section case. A comprehensive analysis to improve the cross section sampling module for these particular cases, will be conduct in the near future.

In the BEAVRS whole benchmark problems, the uncertainties in the design parameters (i.e. CRBW, ITC, FA-wise power distribution, CBC) due to the ^{235}U and ^{238}U cross section uncertainties were generated by the DeCART/MIG UQ analysis code system. The uncertainties in the design parameters were less than the DRC of a typical PWR start-up case, except for the uncertainties in CBCs. This newly-developed DeCART/MIG UQ analysis code system by the S.S. method can be utilized as uncertainty analysis and margin estimation tools to develop and design a new advanced nuclear reactor.

The uncertainties by the DeCART/MIG UQ analysis code system were naturally based on the cross-section covariance data, which were provided by the evaluated nuclear data library vendor. Nowadays, a fully correlated combination of the experimental data, nuclear physical theory, and engineer's evaluation is absent from the covariance data of the evaluated nuclear data library [23]. That

Table 8
Uncertainties in the critical boron concentration due to the ^{235}U and ^{238}U cross section uncertainties for Cycle 1.

EFPD	CBCs and its uncertainties (pcm)	
	Average	Unc.[a]
0	909.9	55.3
4	631.0	53.9
11	615.2	52.9
16	619.3	52.3
22	625.6	51.6
31	630.8	50.5
36	631.0	50.0
52	622.5	48.3
69	602.3	46.7
85	577.3	45.2
96	558.1	44.2
110	531.6	43.1
124	503.6	42.0
141	467.4	40.7
144	461.1	40.5
152	443.3	39.9
164	415.8	39.1
174	392.2	38.4
177	385.1	38.2
180	377.9	38.0
190	353.2	37.3
204	317.8	36.4
214	291.9	35.8
219	278.8	35.5
225	262.9	35.1
228	254.9	34.9
235	235.9	34.5
248	200.0	33.7
271	134.7	32.4
295	65.2	30.7
326	11.2	5.5

[a] Unc. is the absolute uncertainty in CBC due to cross section uncertainties.

Table 9
Uncertainties in the critical boron concentration due to the ^{235}U and ^{238}U cross section uncertainties for Cycle 2.

EFPD	CBCs and their uncertainties (pcm)	
	Average	Unc.[a]
0	1116.3	50.6
13	927.9	47.3
23	894.1	46.5
43	831.4	45.0
63	765.0	43.5
84	693.3	41.9
103	627.5	40.5
129	537.4	38.7
150	464.9	37.4
176	375.5	35.7
202	286.8	34.2
234	178.4	32.5
257	101.1	31.2

[a] Unc. is the absolute uncertainty in CBC due to cross section uncertainties.

may lead to the underestimation or overestimation of the uncertainties in design parameters due to the uncertain covariance data from the evaluated nuclear data library. Therefore, improving the accuracy of the covariance data can upgrade the performance of the DeCART/MIG-provided uncertainties for the nuclear core design analysis.

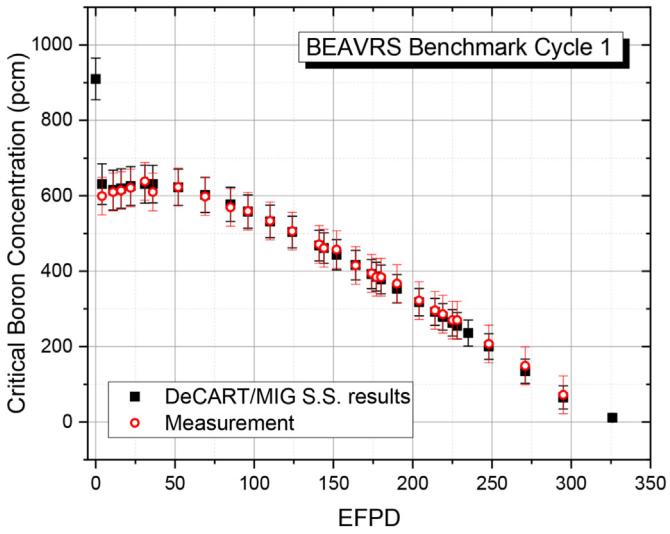

Fig. 6. Uncertainties of the critical boron concentration due to the ^{235}U and ^{238}U cross section uncertainties for Cycle 1.

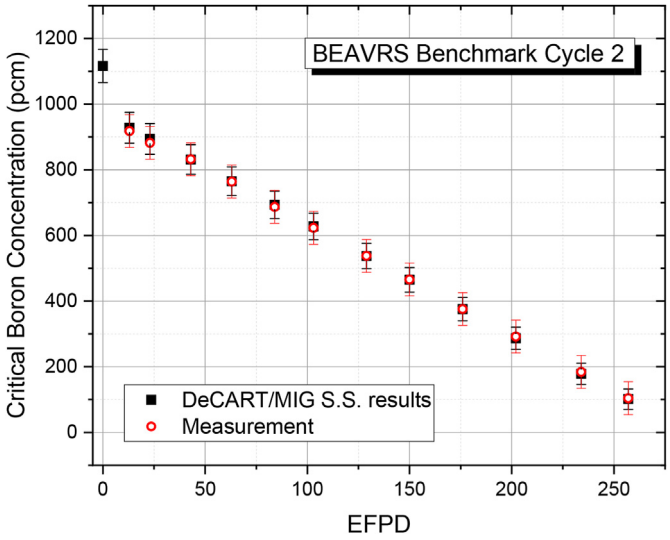

Fig. 7. Uncertainties of the critical boron concentration due to the ^{235}U and ^{238}U cross section uncertainties for Cycle 2.

Declaration of competing interest

The authors declare that they have no known competing financial interests or personal relationships that could have appeared to influence the work reported in this paper.

Acknowledgement

This work was supported by a grant from Kyung Hee University in 2022. (KHU-20220911).

References

[1] J.Y. Cho, et al., DeCART2D v1.1 User's Manual," KAERI/UM-40/2016, Korea Atomic Energy Research Institute, 2016.
[2] J.Y. Cho, et al., MASTER v4.0 User's Manual," KAERI/UM-41/2016, Korea Atomic Energy Research Institute, 2016.
[3] J.Y. Cho, et al., DeCART v1.2 User's Manual," KAERI/TR-3438/2007, Korea Atomic Energy Research Institute, 2007.
[4] C.C. Lee, et al., Some Uncertainties of DeCART2D/MASTER4.0 for 17x17 PWR Core, Transactions of the Korean Nuclear Society Autumn Meeting, Gyeongju, Korea, 2017. October 26-27.
[5] R.P. Martin, A. Petruzzi, Progress in international best estimate Plus uncertainty analysis methodologies, Nucl. Eng. Des. 374 (2021), 111033.
[6] A. Aures, et al., Reactor Simulations with nuclear data uncertainties, Nucl. Eng. Deg. 355 (2019), 110313.
[7] M. Pusa, Incorporating sensitivity and uncertainty analysis to a lattice physics code with application to CASMO-4, Ann. Nucl. Energy 40 (2012) 153–162.
[8] M.L. Williams, et al., A statistical sampling method for uncertainty analysis with SCALE and XSUSA, Nucl. Technol. 183 (2013) 515–526.
[9] A.J. Koning, D. Rochman, Towards sustainable nuclear energy; putting nuclear physics to work, Ann. Nucl. Energy 35 (2008) 2024–2030.
[10] H.J. Park, H.J. Shim, C.H. Kim, Uncertainty propagation in Monte Carlo depletion analysis, Nucl. Sci. Eng. 167 (2011) 196–208.
[11] H.J. Park, et al., Uncertainty propagation analysis for yonggwang nuclear unit 4 by McCARD/MASTER core analysis system, Nucl. Eng. Technol. 46 (2014) 291–298.
[12] T.Y. Han, et al., Development of a sensitivity and uncertainty analysis code for high temperature gas-cooled reactor physics based on the generalized perturbation theory, Ann. Nucl. Energy 85 (2015) 501–511.
[13] T.Y. Han, et al., Improvement and application of DeCART/MUSAD for uncertainty analysis of HTGR neutronic parameters, Nucl. Eng. Technol. 52 (2020) 461–468.
[14] H.J. Park, et al., McCARD/MIG stochastic sampling calculations for nuclear cross section sensitivity and uncertainty analysis, Nucl. Eng. Technol. 54 (2022) 4272–4279.
[15] K. Ivanov, et al., Benchmark for Uncertainty Analysis in Modelling (UAM) for Design, Operation and Safety Analysis of LWRs, Volume I: Specification and Support Data for the Neutronics Cases (Phase I), OECD Nuclear Energy Agency, 2012. NEA/NSC/DOC(2012).
[16] G.K. Delipei, et al., Summary of comparative analysis and conclusions from OECD/NEA LWR-UAM benchmark Phase I, Nucl. Eng. Des. 384 (2021), 111474.
[17] D.N. Horelik, et al., Benchmark for evaluation and validation of reactor Simulations, MIT Computational Reactor Physics Group, Rev03 29 August (2018).
[18] M.B. Chadwick, et al., ENDF/B-VII.1 nuclear data for science and technology: cross sections, covariance, fission product yields and decay data, Nucl. Data Sheets 112 (12) (2011) 2887–2996.
[19] G.E.P. Box, Mervin E. Muller, A note on the generation of random normal deviates, Ann. Math. Stat. 29 (2) (1958) 610–611.
[20] R. Macfarlane, et al., The NJOY Nuclear Data Processing System Version," LA-UR-17-20093, Los Alamos National Laboratory, NW, USA, 2016.
[21] New York Power, Indian Point 3 Nuclear Power Plant Cycle 11 Physics Test Report, New York Power Authority, 2000.
[22] O. Cabellos, et al., Propagation of nuclear data uncertainties for PWR core analysis, Nucl. Eng. Technol. 46 (3) (2014) 299–312.
[23] D.A. Brown, et al., ENDF/B-VIII.0: the 8th major release of the nuclear reaction data library with CIELO-project cross sections, new standards and thermal scattering data, Nucl. Data Sheets 148 (2018) 1–142.